

## Empirical vulnerability curves for Italian residential buildings

A. ROSTI<sup>1</sup>, C. DEL GAUDIO<sup>2</sup>, M. DI LUDOVICO<sup>2</sup>, G. MAGENES<sup>1</sup>, A. PENNA<sup>1</sup>, M. POLESE<sup>2</sup>,  
A. PROTA<sup>2</sup>, P. RICCI<sup>2</sup>, M. ROTA<sup>3</sup> and G.M. VERDERAME<sup>2</sup>

<sup>1</sup> Department of Civil Engineering and Architecture, University of Pavia, Italy

<sup>2</sup> Department of Structures for Engineering and Architecture, University Federico II, Napoli, Italy

<sup>3</sup> Department of Construction and Infrastructure, EUCENTRE Foundation, Pavia, Italy

(Received: 7 March 2019; accepted: 5 December 2019)

**ABSTRACT** This study focuses on the seismic vulnerability assessment of the Italian residential building stock, by taking advantage of post-earthquake damage data collected after past Italian seismic events of the period 1980-2009. Starting from the typological classification of the existing building stock, five vulnerability classes, three for masonry (i.e. A, B, C1) and two for reinforced concrete (i.e. C2 and D) buildings, are identified, grouping buildings exhibiting similar seismic behaviour. Seismic vulnerability is described by correlating empirically-derived damage index (*DI*) values and the peak ground acceleration, representing the selected ground motion intensity measure. To this aim, candidate functional forms are the lognormal and the exponential models. The accuracy of pre-selected functional forms to reproduce the observed seismic *DI* is demonstrated *via* graphical diagnostic and quantified in terms of a coefficient of accuracy. Parameters defining the proposed vulnerability functions are also provided. The results presented in this paper could be used in other regions having similar seismic hazard and built environment.

**Key words:** vulnerability curves, RC and masonry buildings, damage data, building classes, Italian earthquakes.

### 1. Introduction

This study describes the derivation of empirical vulnerability curves for the Italian residential building stock based on the data recently published by the Italian Department of Civil Protection (DPC) in the online platform Da.D.O. [Database di Danno Osservato: Dolce *et al.* (2019)], collecting single-building post-earthquake damage data from Italian earthquakes.

A critical review of this huge amount of damage data is firstly done. As a matter of fact, the procedures managed by Italian DPC to survey damaged buildings may differ for each considered event. Sometimes, post-earthquake inspections are carried out after the explicit request of building's owner only, thus leading to partial and biased samples. Generally speaking, also when a complete survey of the areas most affected by the earthquake is done, buildings' inspections in the surrounding areas are typically restricted to damaged buildings, systematically neglecting the presence of non-damaged buildings. Based on these considerations, the "complete" damage

data are in this work integrated with buildings sited in non-surveyed or partially-surveyed municipalities, to account for the negative evidence of damage at lower levels of ground shaking. Several studies focused on seismic fragility analysis of the Italian building stock (e.g. Braga *et al.*, 1982; Sabetta *et al.*, 1998; Orsini, 1999; Di Pasquale *et al.*, 2005; Rota *et al.*, 2008; Dolce and Goretti, 2015; Zuccaro and Cacace, 2015; Del Gaudio *et al.*, 2017; Rosti *et al.*, 2018). One of the novelties of the present work is represented by the unprecedented availability of post-earthquake data made available by DPC through the Da.D.O. platform. Empirical vulnerability curves for five classes, A, B, and C1 for masonry buildings and C2 and D for reinforced concrete (RC) buildings, are derived for different classes of height, through a nonlinear optimisation procedure with observed damage data. To this aim, different functional forms (i.e. lognormal cumulative distribution and exponential function) are considered and the accuracy of each of them to reproduce the observed damage values is, then, investigated *via* graphical and quantitative diagnostic.

## 2. Damage database

This study takes advantage of post-earthquake damage data collected by the Italian DPC in the Da.D.O. platform (Dolce *et al.*, 2019), assembling information from field surveys on ordinary buildings performed after the main Italian earthquakes occurred in the last 50 years. In particular, the Da.D.O. platform includes nine seismic events of national relevance (i.e. Friuli 1976, Irpinia 1980, Abruzzo 1984, Umbria-Marche 1997, Pollino 1998, Molise 2002, Emilia 2003, L'Aquila 2009, Emilia 2012). The available building parameters concern: i) the identification of the building and its position, ii) general building features (i.e. number of storeys, interstorey height, storey surface area, construction age), iii) typological characteristics (i.e. vertical and horizontal structure types, information on the presence of tie rods or tie beams, if any, of isolated columns, of mixed type structures), iv) damage information detected on different building components.

In spite of some differences on the type and detail of information collected during the different seismic events (e.g. differences in the assumed damage scale, presence or not of information on damage extent and/or on damage to masonry infills/partitions), huge efforts have been very recently undertaken to homogenise all data collected in the Da.D.O. platform (Dolce *et al.*, 2019). On the whole, data on 319,470 ordinary buildings are available, with approximately 78% of masonry buildings, 8% of RC buildings and the remaining part made of other typologies.

The damage database employed in this work includes post-earthquake damage data collected after the Irpinia (1980) and the L'Aquila (2009) earthquakes. Selection of these two seismic events was driven by both the availability of shakemaps and the availability of complete post-earthquake damage data. The ground motion severity was estimated by using shakemaps, consistently derived with the Italian National Institute of Geophysics and Volcanology (INGV) procedure (Michellini *et al.*, 2008). The maps were derived by means of the software package ShakeMap® through the use of different Ground Motion Prediction Equations and the signals registered by the Italian Strong Motion Network (Rete Accelerometrica Nazionale, RAN) and by the Italian National Seismic Network (RSN). INGV reports maps of seismic events with magnitude typically greater than 3 from 2008 to nowadays, implying that only the L'Aquila (2009) and the Emilia (2012) earthquakes could have been considered. Nevertheless, the Emilia (2012) seismic event was discarded due to highly incomplete post-earthquake field surveys. Although not directly available

from the INGV website, the maps of some of the major events occurred before 2008 are reported in Michelini *et al.* (2008), hence allowing to also consider the Irpinia (1980) damage database.

The ground motion severity at the different building locations was represented by the peak ground acceleration (*PGA*). Although alternative seismic intensity measures could have been employed (e.g. Rosti *et al.*, 2020), *PGA* was selected at this stage for the need of complying with the framework of the national seismic risk platform (<http://irma.eucentre.it/irma/web/home>; Borzi *et al.*, 2018).

The *PGA* shakemaps of the 23 November 1980 Irpinia and the 6 April 2009 L'Aquila seismic events are shown in Fig. 1. Uncertainty on the shakemap estimates was neglected, although recognising its importance in the seismic input characterisation. The accuracy of a shakemap indeed varies spatially and it is affected by the availability of nearby ground motion observations, allowing for better constraining the ground shaking in their proximity.

Both the Irpinia and the L'Aquila damage databases also report information about damage on masonry infill/partitions, whose contribution cannot be neglected to properly evaluate seismic capacity of infilled RC frames. This has been also recently highlighted by the analysis of damage data carried out by Dolce and Goretti (2015) and Del Gaudio *et al.* (2016), where the key role played by these components in damage estimation of RC Moment Resisting Frames was emphasised.

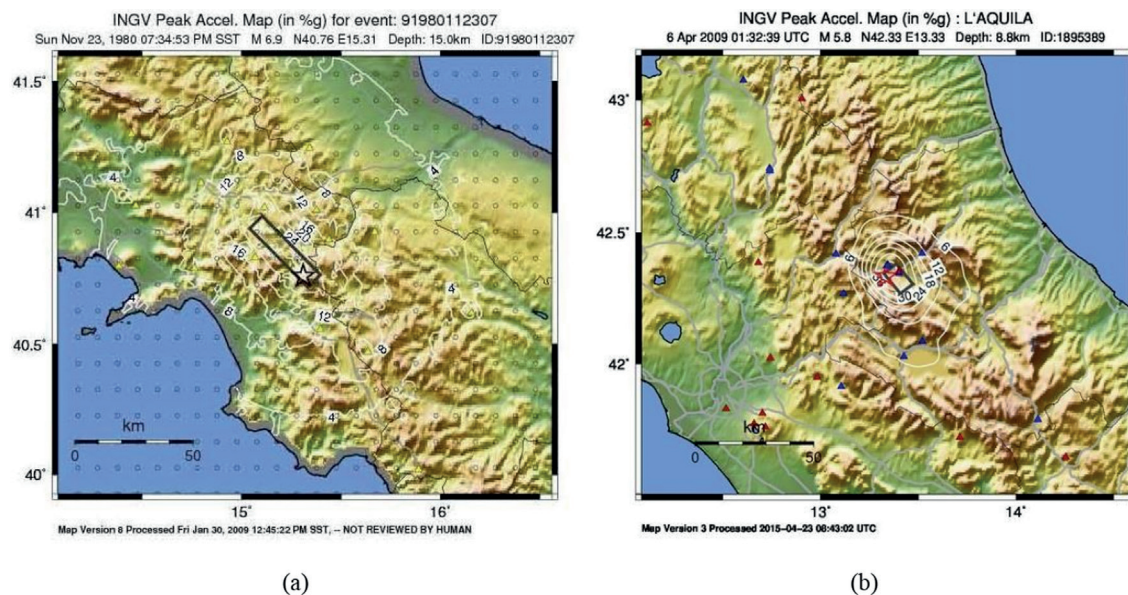


Fig. 1 - Shakemap for the 23 November 1980 Irpinia earthquake (a) from Michelini *et al.* (2008) and for the 6 April 2009 L'Aquila earthquake (b).

### 2.1. Description of the complete damage data sets

All the municipalities reported in the Irpinia database were completely surveyed (Braga *et al.*, 1982). In case of the L'Aquila database, the complete data set was identified by selecting municipalities with completeness (i.e. ratio of the number of surveyed buildings to the total number of buildings) higher than 90%. The total number of residential buildings in each municipality

was retrieved from the national census (ISTAT, 2001). After these filtering procedures, the total number of the residential (i.e. RC and masonry) buildings counted more than 60,000 data. About 39% of these data derives from the Irpinia data set, whereas 61% corresponds to the L'Aquila data set. 10% of the Irpinia data set is constituted by RC constructions, whereas 90% refers to masonry buildings. RC and masonry buildings represent 22% and 78% of the L'Aquila data set, respectively.

About 79% of residential masonry buildings, including data from these two seismic events, are made of irregular layout or poor-quality materials, whereas 21% are characterised by regular texture and good-quality masonry. Classification of the residential masonry building stock of the Irpinia data set shows that 89% and 11% of masonry buildings are low-rise (i.e. 1-2 stories) and mid-/high-rise (i.e. >2 stories), respectively. About 56% of residential masonry buildings of the L'Aquila data set are low-rise, whereas 44% have more than 2 stories. More than 36% of the Irpinia masonry constructions date back prior to 1900, whereas more than 50% of the L'Aquila masonry buildings were built before 1920.

As far as RC buildings are concerned, most of the buildings of the Irpinia 1980 event, for which the information on the age of construction was available, was built after 1962, while for the L'Aquila data set about 34% of the buildings was built before 1981 and 66% after 1981. With regard to the number of stories, 66% of Irpinia data set is between 1 and 2, 30% between 3 and 4, and 4% greater than 4, with a modal value of 2, whereas 29% of the L'Aquila data set is between 1 and 2, 64% between 3 and 4, and 7% greater than 4, with a modal value of 3.

In Figs. 2 and 3, RC and masonry buildings of the Irpinia and L'Aquila data sets are classified based on the number of stories and construction age.

To investigate the representativeness of the considered data set with respect to the Italian residential building stock, some statistics on national building census data are reported in the following. According to ISTAT (2001), the total number of Italian residential buildings is 11,226,595, 61% of which refers to masonry constructions, 25% corresponds to RC buildings, and the remaining 14% to other typologies (i.e. mixed construction, steel, etc.). About 79% of the existing masonry building stock is characterised by low-rise (i.e. 1-2 stories) constructions, whereas 21% is constituted by mid-/high-rise (i.e. >2 stories) buildings. About 66% of the existing

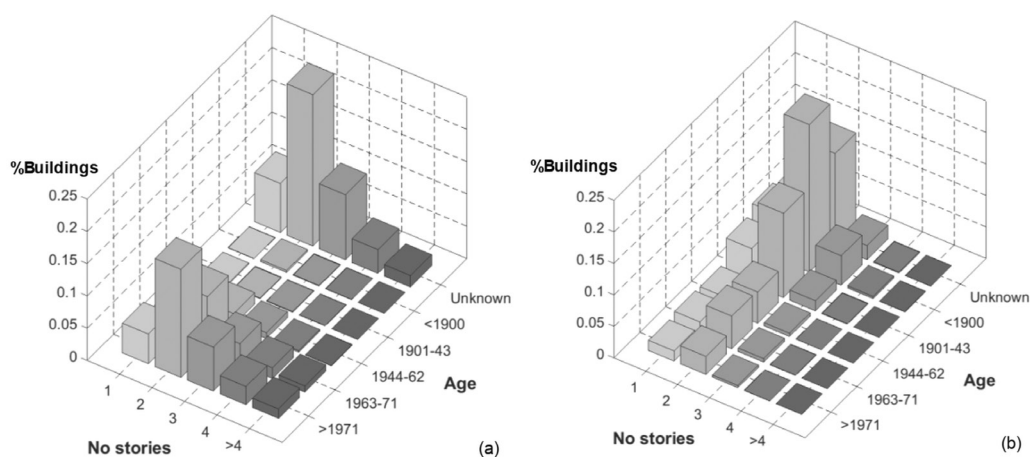


Fig. 2 - Subdivision of the Irpinia RC (a) and masonry (b) building stock based on number of stories and construction age.

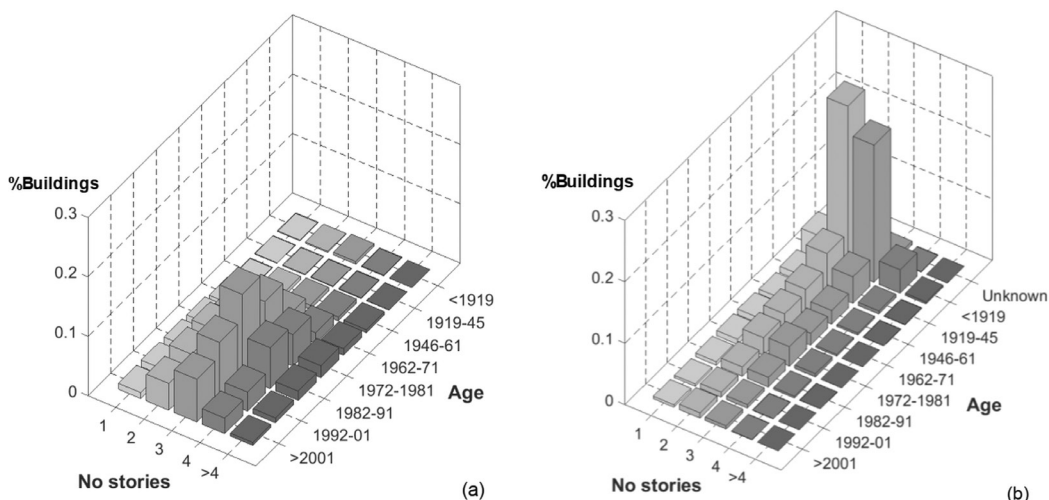


Fig. 3 - Subdivision of the L'Aquila RC (a) and masonry (b) building stock based on number of stories and construction age.

RC building stock is low-rise (i.e. 1-2 stories) whereas 34% has more than two stories. Masonry buildings constructed before 1919 constitute 29% of the masonry existing building stock, whereas modern masonry constructions (construction age >1991) represent 3% of the existing masonry buildings. Conversely, only 3% of RC buildings dates back prior to 1945, whereas 60% was constructed between 1946 and 1981 and 37% thereafter. Figs. 4a and 4b show the regional

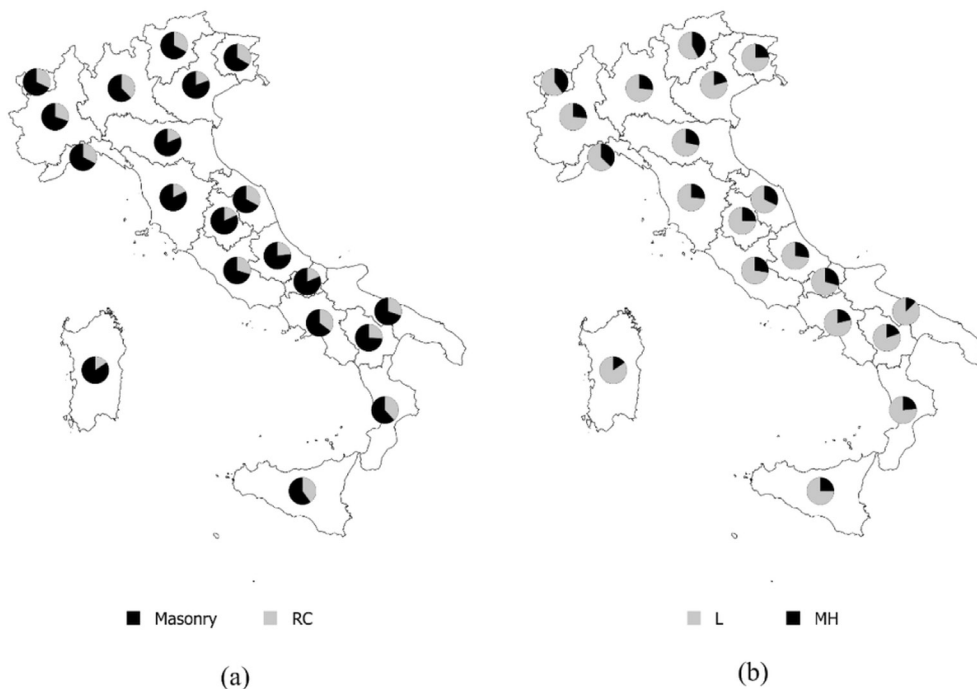


Fig. 4 - Regional distribution of the existing building stock based on construction material (a) and building height (b) according to national census data (ISTAT, 2001).

distribution of residential buildings classified based on construction material (i.e. masonry and RC) and building height (i.e. L: low-rise buildings and MH: mid-/high-rise buildings), respectively.

To account for the negative evidence of damage at lower *PGA* levels, the L'Aquila damage data set was integrated by buildings sited in non-surveyed and partially-surveyed (with completeness lower than 10%) municipalities. The number of residential buildings located in the L'Aquila non-surveyed or partially-surveyed municipalities was retrieved from the national census data (ISTAT, 2001). In case of masonry structures, 136,396 masonry buildings are sited in the 176 non-surveyed municipalities and 38,775 masonry constructions are located in the 49 partially-surveyed municipalities with completeness lower than 10%. On the other hand, for what concerns the L'Aquila RC buildings, 37,861 buildings are sited in the 176 non-surveyed municipalities and 14,641 RC constructions are located in the 49 partially-surveyed municipalities with completeness lower than 10%.

### 3. Damage analysis

Damage classification represents a key issue of seismic fragility assessment. Different procedures, based on either average or maximum seismic damage detected on different building components, are commonly employed for assigning a unique global level of damage to each inspected building (e.g. Rosti *et al.*, 2018). Regardless the adopted approach, the definition of a damage scale and the conversion of the damage description reported in the survey form into discrete damage levels are required. In this work, damage states were defined consistently with the European Macroseismic Scale EMS-98 (Grünthal, 1998). In addition to the absence of damage (DS0), five damage states were identified, i.e. DS1 (slight to negligible damage), DS2 (moderate damage), DS3 (substantial to heavy damage), DS4 (very heavy damage), DS5 (destruction).

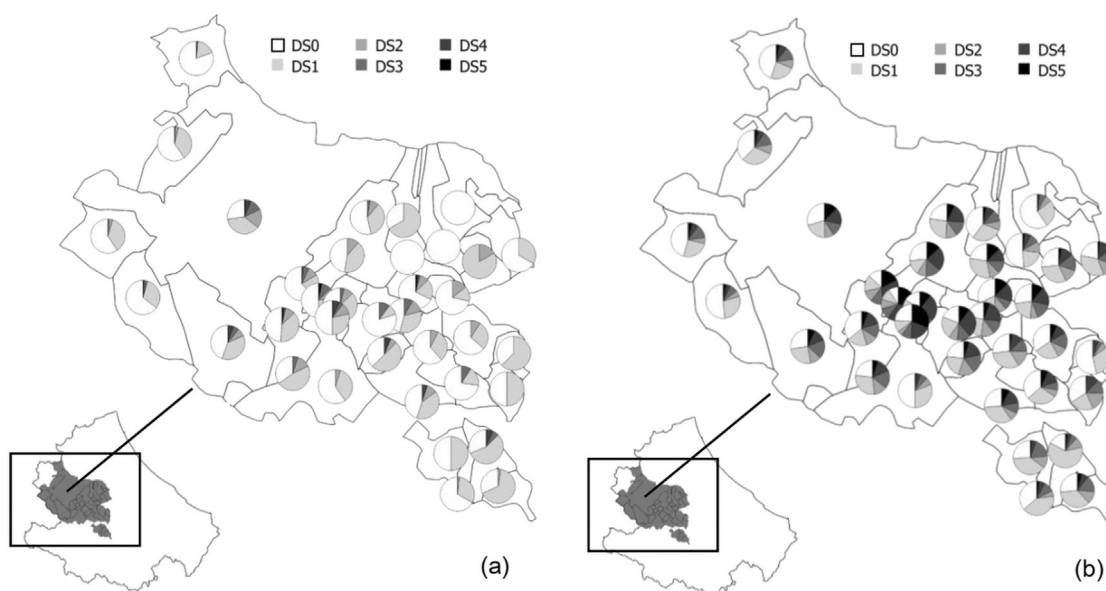


Fig. 5 - Damage classification of RC (a) and masonry (b) buildings of the L'Aquila data set.

The damage description reported in the survey forms was first converted into discrete levels of damage, by adopting the damage conversion rule by Dolce *et al.* (2019), in case of the Irpinia data set, and the Rota *et al.* (2008) and Del Gaudio *et al.* (2017) rules, in case of the L'Aquila survey form for masonry and RC buildings, respectively. The adoption of different damage conversion rules for the two damage databases was necessary, since different post-earthquake survey forms were used in the aftermath of the considered seismic events. A global damage level was, then, assigned to each inspected building, considering the maximum level of damage detected on pre-selected building components. Table 1 reports the adopted damage rules allowing attributing a discrete damage level of the EMS-98 to each damage description, depending on structural and non-structural components. Fig. 5 shows damage classification of RC (Fig. 5a) and masonry (Fig. 5b) buildings of the L'Aquila data set.

Table 1 - Damage conversion rules adopted for damage classification.

EMS-98	Irpinia survey form		L'Aquila survey form	
	Structural components	Non-structural components (RC)	Structural components	Non-structural components (RC)
DS0	No damage	No damage	D0	D0
DS1	Insignificant Negligible	Insignificant Negligible	D1 - <1/3 D1 - 1/3-2/3 D1 - >2/3	D1 - <1/3 D1 - 1/3-2/3 D1 - >2/3
DS2	Considerable Serious	Considerable	D2-D3 - <1/3	D2-D3 - <1/3 D2-D3 - 1/3-2/3 D2-D3 - >2/3
DS3	Very serious	Serious Very serious Partially-collapsed Collapsed	D2-D3 - 1/3-2/3 D2-D3 - >2/3	D4-D5 - <1/3 D4-D5 - 1/3-2/3 D4-D5 - >2/3
DS4	Partially-collapsed		D4-D5 - <1/3 D4-D5 - 1/3-2/3	
DS5	Collapsed		D4-D5 - >2/3	

#### 4. Vulnerability classification

Similarly to existing studies (e.g. Dolce *et al.*, 2003; Lagomarsino and Giovinazzi, 2006; Rosti and Rota, 2017; Rota and Rosti, 2017), seismic damage was globally evaluated at pre-selected *PGA* thresholds in terms of a mean damage index (*DI*), representing the normalised mean damage grade of the damage distribution given the intensity measure, i.e.:

$$DI = \frac{\sum_i d_i f_i}{n} \quad (1)$$

where  $f_i$  is the frequency of occurrence of a given damage state  $d_i$  ( $d_i = 1-5$ ) and  $n$  is equal to 5. The *DI* ranges between 0 and 1, where a *DI* of 0 indicates the absence of damage and *DI* equal to 1 corresponds to collapse.

To provide a continuous description of *DI* as a function of *PGA*, two functional forms were selected, namely the lognormal and the exponential models, also in line with existing studies

focusing on seismic fragility assessment (e.g. Rossetto and Elnashai, 2003; Rota *et al.*, 2008; Del Gaudio *et al.*, 2017). The lognormal and the exponential models, together with the normal cumulative distribution are the most common and widely used for fragility representation (Rossetto *et al.*, 2013).

By using the lognormal distribution, the *DI* trend as a function of *PGA* can be defined as:

$$DI = \Phi \left[ \frac{\ln(PGA/\theta)}{\beta} \right] \quad (2)$$

where  $\Phi[\cdot]$  is the cumulative standard normal distribution,  $\theta$  is the median and  $\beta$  the logarithmic standard deviation, respectively.

In addition to the lognormal distribution, the exponential model was also selected. In this case, the *DI* trend as a function of *PGA* can be defined as:

$$DI = 1 - e^{-\gamma PGA^\delta} \quad (3)$$

where  $\gamma$  and  $\delta$  are the parameters defining the exponential model, considering *PGA* in g units.

Both the selected functional forms were fitted to the empirical data points through a nonlinear fitting procedure minimising the sum of the weighted squared errors. Given that the reliability of each observational data point is affected by the sample size (i.e. number of buildings in each predefined *PGA* interval), the weighted form of the least squares approach allowed to limit the effect of less reliable data points in the model fitting. To this aim, a weight, represented by the total number of buildings within a given *PGA* interval, was associated to the corresponding empirical *DI* value.

#### 4.1. Typological vulnerability curves for masonry building typologies

Masonry buildings were allocated to eight building typologies representative of the Italian building stock. Building typologies were identified based on the typological information collected in the post-earthquake survey forms, such as layout and quality of the masonry fabric (i.e. irregular layout or poor-quality masonry and regular layout and good-quality masonry), in-plane flexibility of the intermediate diaphragms (i.e. flexible and rigid) and presence of connecting devices (i.e. tie-rods and/or tie-beams). Given that two different survey forms were adopted for seismic damage assessment after the Irpinia and L'Aquila earthquakes, an intermediate process of data homogenisation was first required. The typological classification system adopted for masonry buildings is reported in Table 2, whilst in Fig. 6 masonry constructions are subdivided into the predefined building typologies. Data statistics refer to the damage data set. As discussed in section 2.1, damage data were, then, integrated by undamaged buildings, whose number was identified, for each municipality, from national census. As the only building attributes considered by the national census data are construction material, construction age and number of stories, masonry buildings from national census were mapped to the predefined building typologies based on the representativeness (i.e. frequency) of each building typology within the considered post-earthquake damage data set. For RC buildings, this assumption was not required, as the mapping was straightforward.

Table 2 - Typological classification system adopted for masonry buildings.

Masonry layout and quality	Type of diaphragm	Presence of tie-rods and/or tie-beams	Label
Irregular layout or poor-quality (IRR)	Flexible (F)	No Yes	IRR_F_NCD IRR_F_CD
	Rigid (R)	No Yes	IRR_R_NCD IRR_R_CD
Regular layout and good-quality (REG)	Flexible (F)	No Yes	REG_F_NCD REG_F_CD
	Rigid (R)	No Yes	REG_R_NCD REG_R_CD

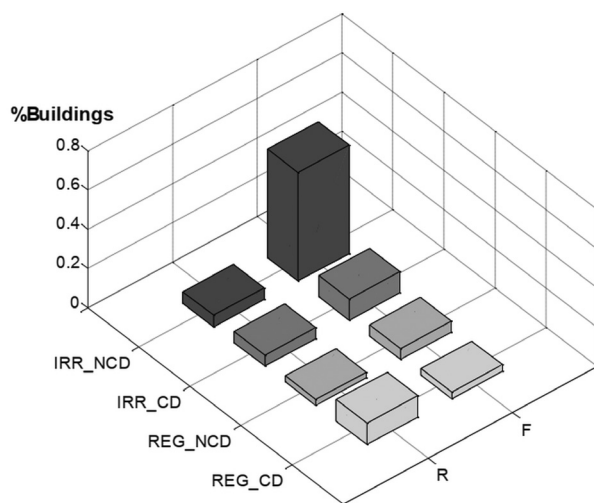


Fig. 6 - Typological classification of masonry buildings.

Empirically-derived *DI* values are shown in Fig. 7 for pre-selected *PGA* thresholds and masonry building typologies.

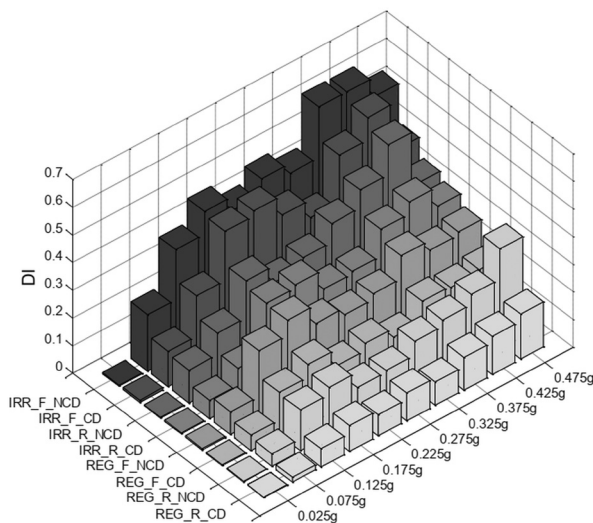


Fig. 7 - *DI* values as a function of *PGA* thresholds for predefined building typologies.

Fig. 8 shows empirically-derived *DI* curves as a function of *PGA*, for masonry building typologies. Curves of pre-selected building typologies, obtained from pre-selected functional forms, are superimposed in Fig. 9. Irregular layout or poor-quality masonry constructions exhibit significantly higher seismic vulnerability than the corresponding building typology with regular texture and good-quality masonry. The presence of connecting devices, such as tie-rods and/or tie-beams, reduces seismic vulnerability. Focusing on the in-plane flexibility of the intermediate horizontal structures, rigid diaphragms are less vulnerable than flexible ones. The natural aggregation of building typologies into vulnerability classes is also evident from the comparison of vulnerability curves for the identified structural typologies.

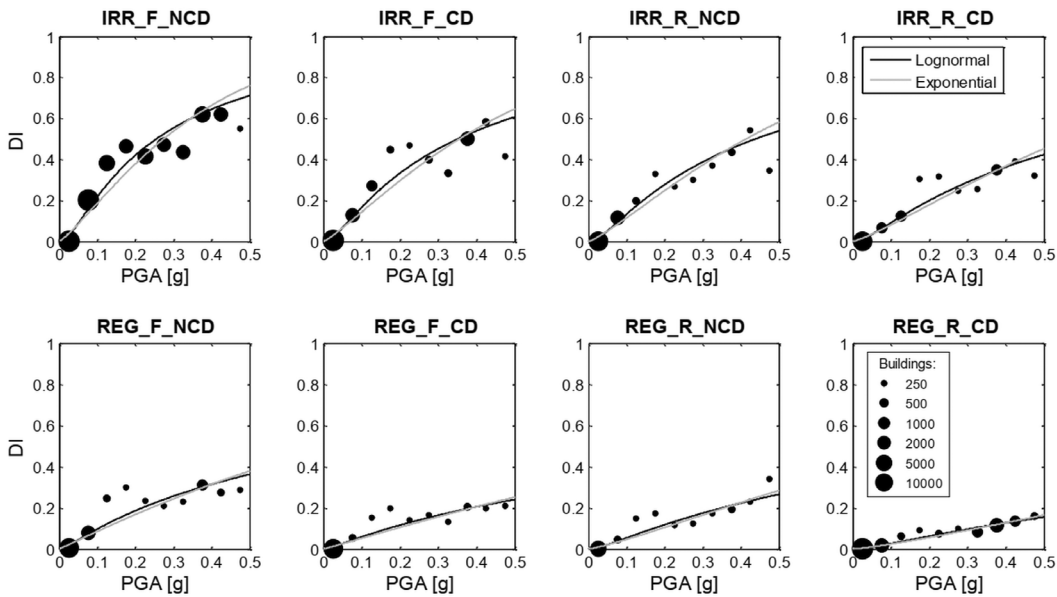


Fig. 8 - *DI* curves for masonry building typologies.

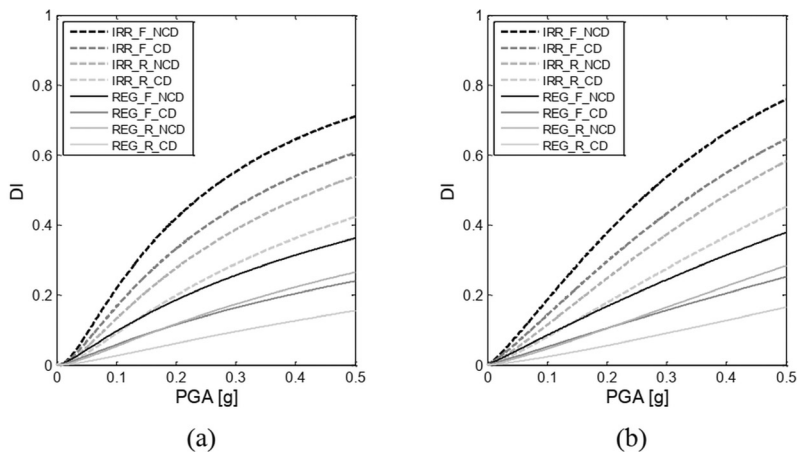


Fig. 9 - Comparison of *DI* curves for masonry buildings considering different building typologies and functional forms: a) lognormal; b) exponential model.

#### 4.2. Typological vulnerability curves for RC building typologies

RC buildings are firstly allocated as a function of the type of design (i.e. for gravity loads only, for seismic loads pre-1981 deemed as “obsolete”, and for seismic loads post-1981). Roughly speaking, data on buildings designed for gravity loads only or for seismic loads derive from the Irpinia 1980 and the L’Aquila 2009 event, respectively, because most of municipalities hit by the Irpinia event were not yet classified as seismic in 1980, whereas most of the municipalities stricken by the L’Aquila earthquake were classified as seismic since 1915 (R.D.L. 29/04/1915 n. 573, 2015). The choice of distinguishing between pre- and post-1981 seismically designed buildings was based, on one side, on the evolution of technical codes (D.M. 03/03/1975, 1975) and, on the other side, on the need of consistency between the databases of the two events.

Fig. 10 shows empirically-derived  $DI$  curves as a function of  $PGA$ , for RC building typologies. The trend of the  $DI$  curves of RC buildings designed for gravity loads only and those with seismic design pre-1981 is affected by the amount of data in the different  $PGA$  bins. However, where the size of the available samples is comparable, the two building typologies exhibit similar seismic vulnerability and, therefore, they will be grouped together, as discussed in Section 4.3.

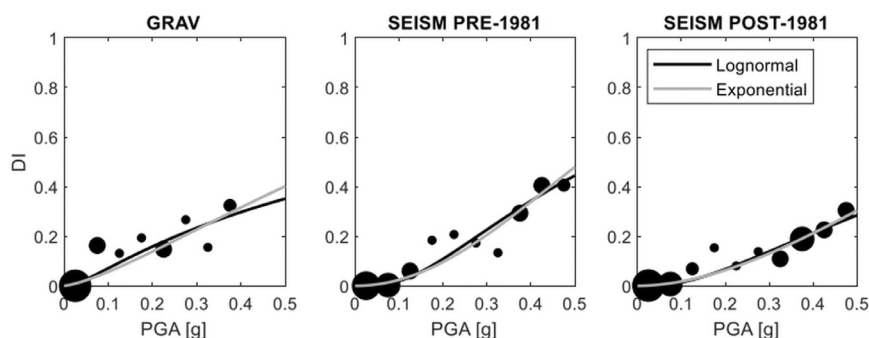


Fig. 10 -  $DI$  curves for RC building typologies.

#### 4.3. Derivation of class vulnerability curves

Starting from the typological classification of the building stock, five vulnerability classes of decreasing vulnerability were defined: vulnerability classes A, B, and C1 correspond to masonry constructions with decreasing vulnerability, whereas vulnerability classes C2 and D correspond to RC buildings with decreasing vulnerability. The association of building typologies to vulnerability classes makes the proposed empirical model easily usable and applicable when general information on building characteristics is available. Furthermore, the definition of five vulnerability classes is consistent with the structure of the Italian national platform for territorial seismic risk assessment (<http://irma.eucentre.it/irma/web/home>; Borzi *et al.*, 2018). The association of masonry building typologies to vulnerability classes A, B, and C1, of decreasing vulnerability, was carried out based on the similarity of the observed seismic fragility, by implementing an agglomerative hierarchical clustering procedure (e.g. Day and Edelsbrunner, 1984). The similarity between building typologies was quantified in terms of a distance metric, allowing to iteratively merge building typologies with shortest inter-distance into wider clusters. The procedure was repeated until three classes (i.e. vulnerability classes A, B, and C1) were obtained. Outcome of the adopted

clustering strategy is reported in Table 3, indicating the building typologies pertaining to the predefined vulnerability classes.

For each vulnerability class, values of *DI* were, then, computed for pre-selected *PGA* thresholds (Fig. 11a). In Fig. 11b *DI* values are computed for vulnerability classes accounting for the building class of height, i.e. L: low-rise buildings (1-2 stories) and MH: mid-/high-rise buildings (>2 stories).

Table 3 - Definition of vulnerability classes for masonry buildings.

Class A	Class B	Class C1
IRR_F_NCD	IRR_R_CD	REG_F_CD
IRR_F_CD	REG_F_NCD	REG_R_NCD
IRR_R_NCD		REG_R_CD

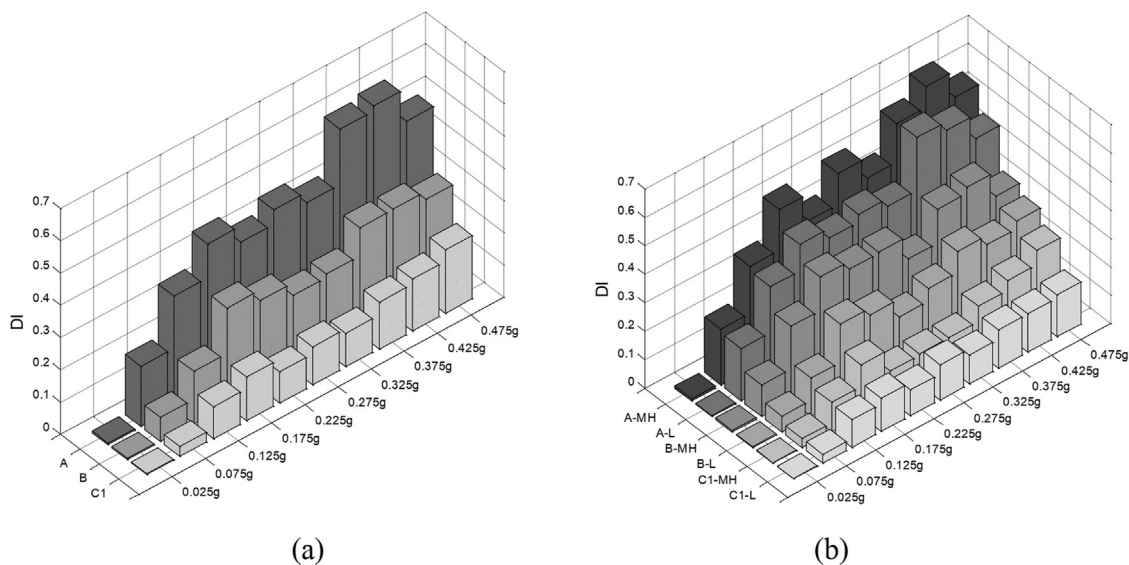


Fig. 11 - *DI* values as a function of *PGA* thresholds for predefined vulnerability classes for masonry buildings (a) and vulnerability classes and class of height (b).

Consistently with the aforementioned procedure, empirically-derived curves, correlating the observed *DI* with *PGA*, were derived for vulnerability classes A, B, and C1 and two functional forms (Fig. 12). In Fig. 13, vulnerability classes are refined based on the building class of height, i.e. L: low-rise buildings (1-2 stories) and MH: mid-/high-rise buildings (>2 stories).

RC buildings were mapped to vulnerability classes C2 and D, of decreasing vulnerability, based on the level of design, accounting for code evolution. RC buildings designed for gravity loads only or for seismic loads pre-1981 were attributed to vulnerability class C2, whereas buildings designed for seismic loads post-1981 were assigned to vulnerability class D.

Empirically-derived curves for vulnerability classes C2 and D as a function of the considered two functional forms are reported in Fig. 14. In Fig. 15, vulnerability classes are refined based

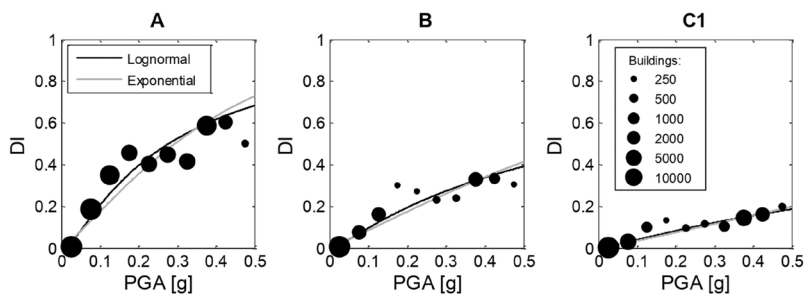


Fig. 12 - Vulnerability curves for vulnerability classes A, B, and C1.

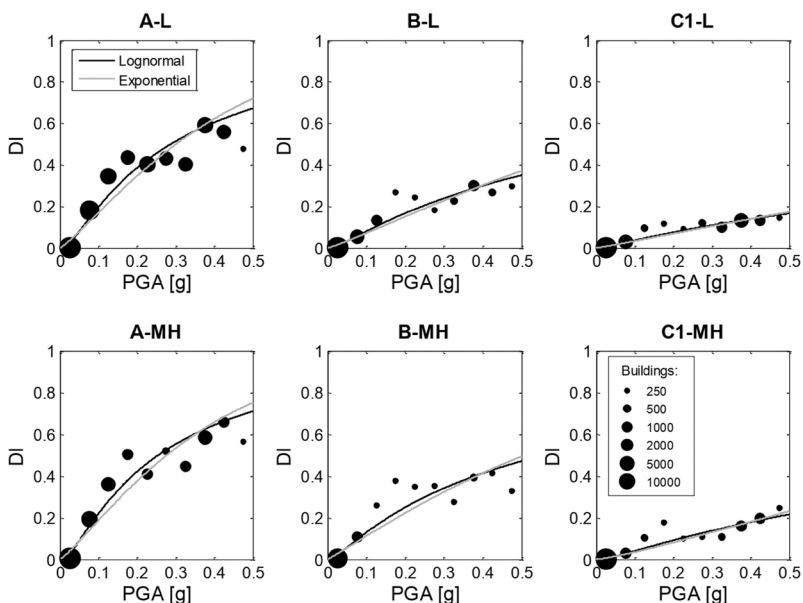


Fig. 13 - Vulnerability curves for vulnerability classes A, B, and C1 and classes of story L (1 - 2 stories) and MH (>2 stories).

on the building class of height, i.e. L: low-rise buildings (1-2 stories) and MH: mid/high-rise buildings (>2 stories).

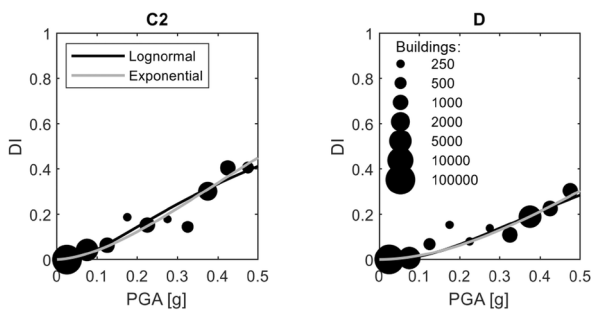


Fig. 14 - Vulnerability curves for vulnerability classes C2 and D.

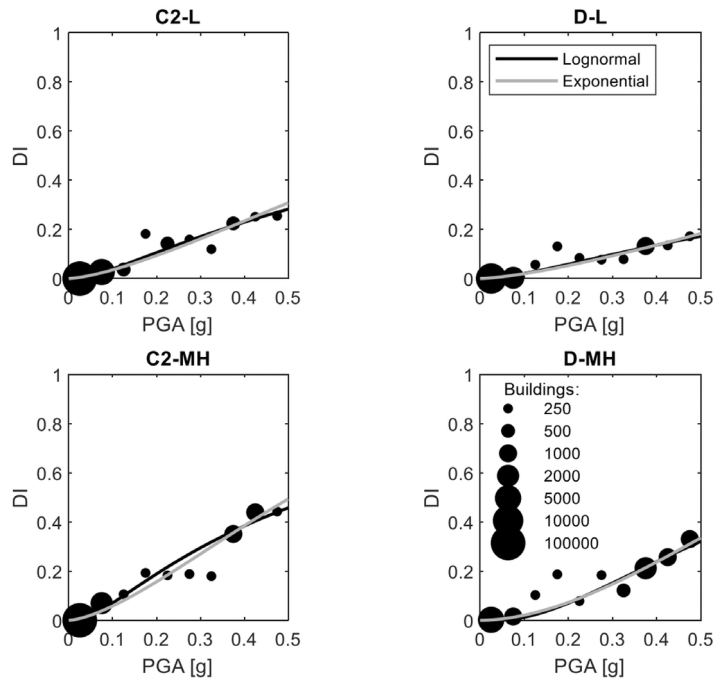


Fig. 15 - Vulnerability curves for vulnerability classes C2 and D and classes of story L (1-2 stories) and MH (>2 stories).

The goodness-of-fit was graphically assessed by plotting the predicted *DI* values against the observational ones (Fig. 16). The accuracy of each selected model to reproduce the observed *DI* values was also globally quantified in terms of the coefficient of efficiency, *E* (Nash and Sutcliffe, 1970):

$$E = 1 - \frac{\sum_{i=1}^n (y_i - \hat{y}_i)^2}{\sum_{i=1}^n (y_i - \bar{y})^2} \tag{4}$$

where  $y_i$  are the observations,  $\hat{y}_i$  indicate the predictions,  $\bar{y}$  is the mean of the observations and  $n$  is the total number of observations. The coefficient of efficiency is a measure of the dispersion with respect to the bisector line, indicating that predictions perfectly match observations.

Results show that the coefficient of efficiency exceeds 80% in all the cases, suggesting the suitability of both the lognormal and exponential models to reproduce the observational *DI* values (Fig. 16). However, higher efficiency is globally attained when the lognormal model is adopted.

Table 4 reports the parameters of the lognormal and exponential models, respectively, to derive *DI* curves as a function of *PGA* for predefined vulnerability classes. Starting from the proposed vulnerability curves in terms of mean damage, for a given *PGA* threshold the overall damage distribution could be also derived under the assumption of binomial distribution (e.g. Braga *et al.*, 1982; Lagomarsino and Giovinazzi, 2006).

Figs. 17 and 18 compare observational damage frequencies of vulnerability classes A and C2 (selected as examples) with those estimated by the binomial distribution (black line). In line with existing studies (e.g. Sabetta *et al.*, 1998; Rosti *et al.*, 2018), the binomial model allows to well approximate empirical DPMs (Damage Probability Matrices) in some cases (Fig. 18), whereas, in other cases, its limited flexibility does not permit to well reproduce damage repartition in

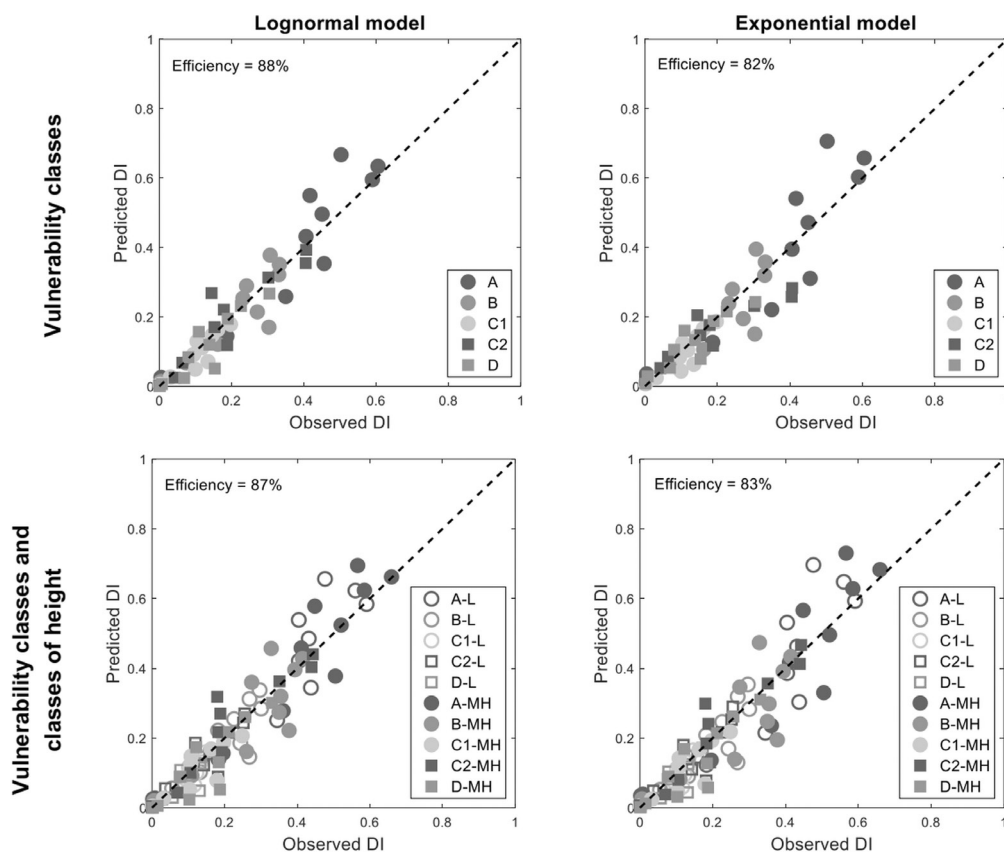


Fig. 16 - Diagnostic plots graphically assessing the goodness-of-fit for the lognormal and exponential models for vulnerability classes and vulnerability classes and class of height.

Table 4 - Parameters of *DI* curves as a function of *PGA* for vulnerability classes (L: 1-2 stories, MH: >2 stories, All: all stories).

Vulnerability class	Class of height	Lognormal model		Exponential model*	
		$\theta$ [g]	$\beta$ [-]	$\gamma$ [-]	$\delta$ [-]
A	L	0.288	1.244	2.901	1.195
	MH	0.256	1.216	3.169	1.187
	All	0.278	1.237	2.974	1.192
B	L	0.919	1.574	1.022	1.143
	MH	0.560	1.516	1.442	1.088
	All	0.771	1.555	1.161	1.125
C1	L	3.358	1.959	0.402	1.078
	MH	1.867	1.672	0.623	1.249
	All	2.559	1.828	0.485	1.148
C2	L	1.095	1.360	1.001	1.443
	MH	0.567	1.181	1.935	1.509
	All	0.639	1.095	1.880	1.654
D	L	2.010	1.473	0.545	1.431
	MH	0.762	0.907	1.462	1.839
	All	0.878	0.988	1.324	1.870

\* The parameters of the exponential model apply to *PGA* in g units

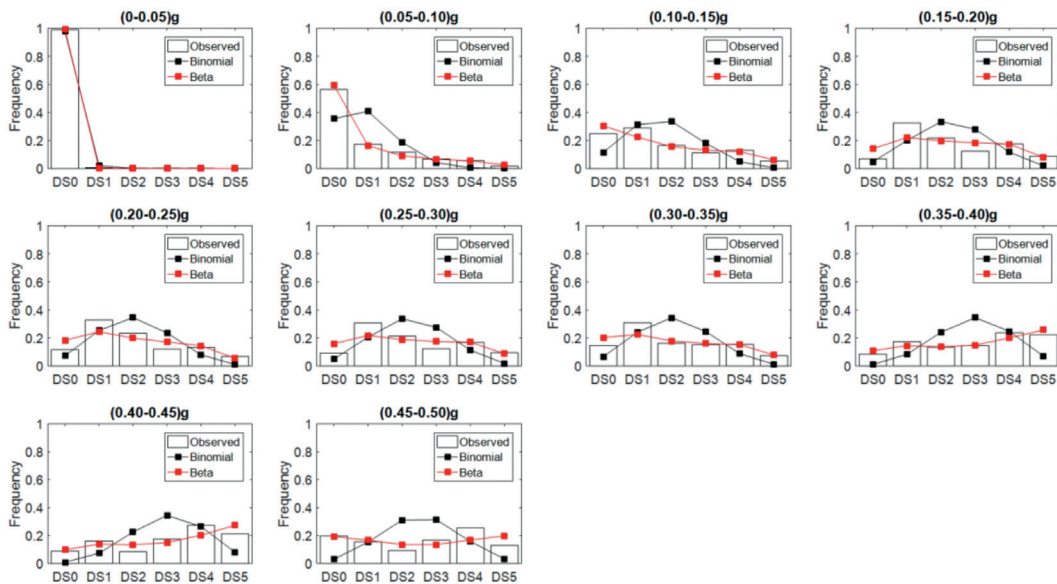


Fig. 17 - Comparison of observational damage frequencies with the predicted ones assuming binomial (black) and beta (red) distributions. Vulnerability class A - All.

the different damage levels (Fig. 17). Being more versatile than the binomial model, the beta distribution (red line in Figs. 17 and 18) better approximates empirical damage distributions, as also demonstrated by other literature studies (e.g. Lagomarsino and Giovinazzi, 2006; Lallemand and Kiremidjian, 2015). Despite its limited flexibility, the advantage of the binomial model is, however, the fact that damage repartition in the different damage states can be described through a unique parameter, representing the mean damage of the discrete distribution.

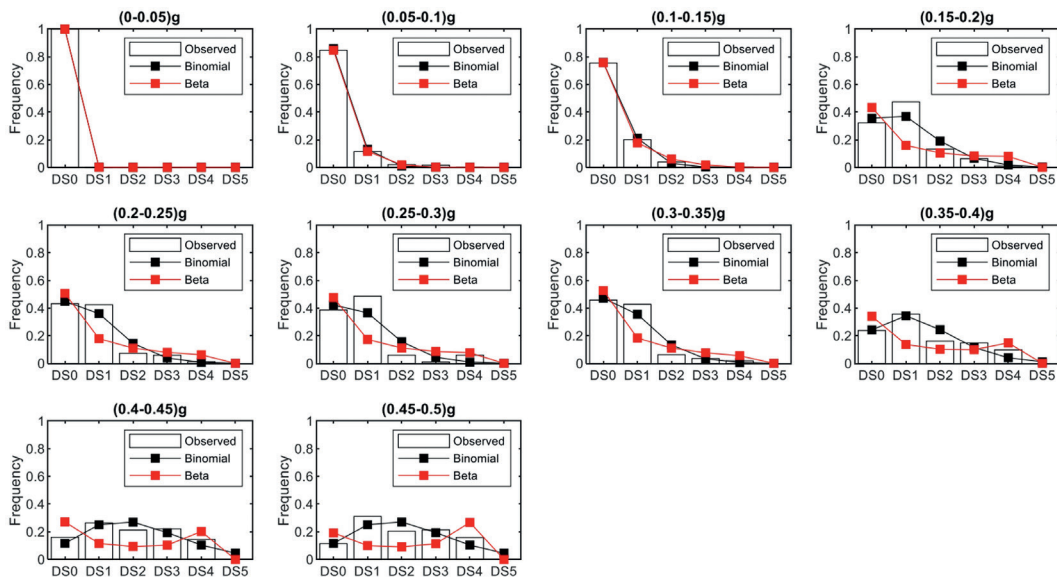


Fig.18 - Comparison of observational damage frequencies with the predicted ones assuming binomial (black) and beta (red) distributions. Vulnerability class C2 - All.

## 5. Conclusions

This paper presents empirically-derived seismic vulnerability curves for vulnerability classes, by statistically processing post-earthquake damage data collected in the aftermath of the Irpinia (1980) and L'Aquila (2009) events. The derivation of vulnerability curves first required the selection of a ground motion intensity measure, the classification of the observed seismic damage and the adoption of a typological classification system. Starting from the typological classification of the Italian residential building stock, five vulnerability classes were identified, three for masonry (i.e. A, B, and C1) and two for RC (i.e. C2 and D) buildings. Pre-defined vulnerability classes were, then, refined based on the building class of height, i.e. L: low-rise buildings (1-2 stories) and MH: mid-/high-rise buildings (>2 stories). Similarly to existing studies (e.g. Dolce *et al.*, 2003; Lagomarsino and Giovinazzi, 2006), the *DI* was selected as global damage indicator and empirical vulnerability curves were derived by fitting the lognormal and exponential models to observational *DI* values. Graphical diagnostic was carried out to assess the goodness-of-fit of the empirically-derived vulnerability curves. The capability of the selected functional forms to reproduce empirical data points was also globally quantified in terms of a coefficient of efficiency. Although the lognormal model globally led to more accurate predictions than the exponential model, results generally showed that both the pre-selected functional forms can satisfactorily reproduce observational *DI* values, with values of the coefficient of efficiency higher than 80%. The performance of the proposed vulnerability models to reproduce observed seismic damage could be tested in the future by using post-earthquake damage data from other seismic events.

The vulnerability model proposed in this work could be used for simulating seismic damage scenarios and for territorial seismic risk applications. If implemented in a GIS environment, it could be also useful for supporting post-earthquake emergency actions in the aftermath of a seismic event, allowing for rapid evaluations of the spatial distribution of damage and for the identification of the most affected territories, where emergency interventions should be prioritised.

The presented empirical model was derived as a function of *PGA* to meet the main characteristics of the national seismic risk platform. The use of alternative intensity measures, for which both seismic hazard studies and shakemaps are available, will be investigated in the future, by setting up an *ad hoc* study for identifying the intensity measures better correlated with the observed seismic damage.

**Acknowledgements.** This study was developed under the financial support of the Italian DPC, within the ReLUIS - DPC 2014-2018 project. This support is gratefully acknowledged. This study represents an advancement of that presented at 37th National Conference of GNGTS (Gruppo Nazionale di Geofisica della Terra Solida), Bologna, 19-21 November 2018.

## REFERENCES

- Borzi B., Faravelli M., Onida M., Polli D., Quaroni D., Pagano M. and Di Meo A.; 2018: *IRMA Platform (Italian Risk Maps)*. In: Proc., 37th National Conference GNGTS, Bologna, Italy, pp. 382-386.
- Braga F., Dolce M. and Liberatore D.; 1982: *A statistical study on damaged buildings and an ensuing review of the M.S.K.-76 scale*. In: Proc., 7th European Conference on Earthquake Engineering, Athens, Greece, pp. 431-450.
- D.M. 03/03/1975; 1975: *Decreto Ministeriale "Approvazione delle norme tecniche per le costruzioni in zone sismiche"*. Gazzetta Ufficiale della Repubblica Italiana 08/04/1975, Roma, Italy, n. 93.
- Day W.H.E. and Edelsbrunner H.; 1984: *Efficient algorithms for agglomerative hierarchical clustering methods*. J. Classification, 1, 7-24.

- Del Gaudio C., Ricci P., Verderame G.M. and Manfredi G.; 2016: *Observed and predicted earthquake damage scenarios: the case study of Pettino (L'Aquila) after the 6th April 2009 event*. Bull. Earthquake Eng., **14**, 2643-2678, doi: 10.1007/s10518-016-9919-2.
- Del Gaudio C., De Martino G., Di Ludovico M., Manfredi G., Prota A., Ricci P. and Verderame G.M.; 2017: *Empirical fragility curves from damage data on RC buildings after the 2009 L'Aquila earthquake*. Bull. Earthquake Eng., **15**, 1425-1450.
- Di Pasquale G., Orsini G. and Romeo R.W.; 2005: *New developments in seismic risk assessment in Italy*. Bull. Earthquake Eng., **3**, 101-128.
- Dolce M. and Goretti A.; 2015: *Building damage assessment after the 2009 Abruzzi earthquake*. Bull. Earthquake Eng., **13**, 2241-2264.
- Dolce M., Masi A., Marino M. and Vona M.; 2003: *Earthquake damage scenarios of the building stock of Potenza (southern Italy) including site effects*. Bull. Earthquake Eng., **1**, 115-140.
- Dolce M., Speranza E., Giordano F., Borzi B., Bocchi F., Conte C., Di Meo A., Faravelli M. and Pascale V.; 2019: *Observed damage database of past Italian earthquakes: the Da.D.O. Webgis*. Boll. Geof. Teor. Appl., **60**, 141-164.
- Grünthal G. (ed); 1998: *European Macroseismic Scale 1998*. Cahiers du Centre Européen de Géodynamique et de Séismologie, Luxembourg, **7**, 99 pp.
- ISTAT; 2001: *General census on population and housing*. Roma, Italy, <www.Dati.Istat.it>.
- Lagomarsino G. and Giovinazzi S.; 2006: *Macroseismic and mechanical models for the vulnerability and damage assessment of current buildings*. Bull. Earthquake Eng., **4**, 415-443.
- Lallemant D. and Kiremidjian A.; 2015: *A beta distribution model for characterizing earthquake damage state distribution*. Earthquake Spectra, **31**, 1337-1352.
- Michelini A., Faenza L., Lauciani V. and Malagnini L.; 2008: *ShakeMap implementation in Italy*. Seismol. Res. Lett., **79**, 688-697.
- Nash J.E. and Sutcliffe J.V.; 1970: *River flow forecasting through conceptual models: Part I, a discussion of principles*. J. Hydrol., **10**, 282-290.
- Orsini G.; 1999: *A model for buildings' vulnerability assessment using the Parameterless Scale of Seismic Intensity (PSI)*. Earthquake Spectra, **15**, 463-483.
- R.D.L. 29/04/1915 n. 573; 1915: *Regio Decreto Legge "Norme tecniche ed igieniche da osservarsi per i lavori edilizi nelle località colpite dal terremoto del 13/01/1915"*. Gazzetta Ufficiale della Repubblica Italiana 11/05/1915, Roma, Italy, n. 117.
- Rossetto T., Ioannou I. and Grant D.N.; 2013: *Existing empirical fragility and vulnerability functions: compendium and guide for selection*. GEM Foundation, Pavia, Italy, GEM Technical Report 2013-X, 62 pp.
- Rosti A. and Rota M.; 2017: *Comparison of PSH results with historical macroseismic observations at different scales - Part 2: applications to south-east France*. Bull. Earthquake Eng., **15**, 4609-4633.
- Rosti A., Rota M. and Penna A.; 2018: *Damage classification and derivation of damage probability matrices from L'Aquila (2009) post-earthquake survey data*. Bull. Earthquake Eng., **16**, 3687-3720.
- Rosti A., Rota M. and Penna A.; 2020: *Influence of seismic input characterization on empirical damage probability matrices from the 2009 L'Aquila event*. Soil Dyn. Earthquake Eng., **128**, 105870, 15 pp., doi: 10.1016/j.soildyn.2019.105870.
- Rota M. and Rosti A.; 2017: *Comparison of PSH results with historical macroseismic observations at different scales - Part 1: methodology*. Bull. Earthquake Eng., **15**, 4585-4607.
- Rota M., Penna A. and Strobbia C.L.; 2008: *Processing Italian damage data to derive typological fragility curves*. Soil Dyn. Earthquake Eng., **28**, 933-947.
- Sabetta F., Goretti A. and Lucantoni A.; 1998: *Empirical fragility curves from damage surveys and estimated strong ground motion*. In: Proc., 11th European Conference on Earthquake Engineering, Paris, France, 11 pp.
- Zuccaro G. and Cacace F.; 2015: *Seismic vulnerability assessment based on typological characteristics. The first level procedure "SAVE"*. Soil Dyn. Earthquake Eng., **69**, 262-269.

Corresponding author: Marco Di Ludovico  
Department of Structures for Engineering and Architecture, University Federico II  
Via Claudio 21, 80125 Napoli, Italy  
Phone: +39 081 7683900; e-mail: diludovi@unina.it